

# Configuration-interaction method with Hylleraas-Gaussian-type basis functions in cylindrical coordinates: Helium atom in a strong magnetic field

Xiaofeng Wang and Haoxue Qiao

*Department of Physics, Wuhan University, Wuhan 430072, China*

(Received 22 January 2008; published 22 April 2008)

The energy levels involving the  $^10^+$ ,  $^1(-1)^+$ , and  $^1(-2)^+$  states of the helium atom in strong magnetic fields up to  $2.35 \times 10^7$  T are investigated. Our computational approach is a configuration-interaction (CI) method based on a set of anisotropic Hylleraas-Gaussian orbitals nonlinearly optimized for different field strength. A detailed comparison between our method and the CI method with the Gaussian-type basis functions in cylindrical coordinates is made. The advantages of the Hylleraas-Gaussian basis over the Gaussian basis are discussed.

DOI: [10.1103/PhysRevA.77.043414](https://doi.org/10.1103/PhysRevA.77.043414)

PACS number(s): 32.60.+i, 32.30.-r, 32.70.-n

## I. INTRODUCTION

The discovery of the existence of huge magnetic fields in white dwarf stars ( $10^2$ – $10^5$  T) and neutron stars ( $10^7$ – $10^9$  T) [1], and the observations of excitons with small effective masses and large dielectric constants in semiconductors [2] or quantum dots [3], have stimulated lasting research interests in the theoretical study of atomic systems in strong magnetic fields. Under these extreme conditions, the electrons experience electric and magnetic forces of comparable strength and the magnetic field cannot be treated as a small perturbation. Rösner *et al.* [4] has done detailed work on the spectrum of the hydrogen atom in strong magnetic fields, which has been successfully applied to the identification of the spectra from many magnetic white dwarf stars [5]. Up to now, much accurate data about the hydrogen atom in strong magnetic fields is available for astronomical observation [6–16]. However, the spectra from many magnetic white dwarf stars cannot be completely accounted for with hydrogen [17,18]. Therefore, detailed studies of heavier atoms in strong magnetic fields are necessary. Ivanov investigated the energy levels of the helium atom in magnetic fields via a Hartree-Fock mesh approach [19]. In Ref. [20], Scrinzi calculated the bound-state energies of the helium atom in magnetic fields with Hylleraas-type explicitly correlated functions in spherical coordinates, and results with high precision are obtained only in weak and intermediate magnetic fields. Hesse *et al.* [21] calculated the energy levels of the helium atom in strong magnetic fields with a Lagrange-mesh method. Using a full configuration-interaction (CI) approach based on a nonlinearly optimized anisotropic Gaussian basis set of one-particle functions, Becken *et al.* have investigated the electronic structure of the helium atom in strong magnetic fields [22–24], and using the data they provided, Jordan *et al.* have proved that the mysterious absorption edges of the magnetic white dwarf GD229 attributes to helium in a strong magnetic field of  $B \approx 50\,000$  T [25,26].

In the case of strong magnetic fields, the spherical symmetry is mostly broken and a basis set with cylindrical symmetry is more applicable. Aiming at increasing the accuracy in cylindrical coordinates, we adopt a CI method with a Gaussian-Hylleraas-type basis set for the calculation of the helium atom in strong magnetic fields. Section II contains a description of the Hamiltonian and the trial wave function.

The energy levels are presented in Sec. III, in which our results are mainly compared with the corresponding data in Refs. [22–24], as are CI calculations in cylindrical coordinates. Concluding remarks are given in Sec. IV. The overlap matrix elements, as well as the Hamiltonian matrix elements, are given in the Appendix. Atomic units are used throughout.

## II. THEORY AND METHOD

Assuming that the nuclear mass is infinite and the magnetic field is in the  $z$  direction, the nonrelativistic Hamiltonian of a two-electron system in a magnetic field can be expressed in cylindrical coordinates as

$$H = \sum_{i=1}^2 \left[ \frac{1}{2} \left( p_i + \frac{1}{2} \mathbf{B} \times \mathbf{r}_i \right)^2 - \frac{Z}{r_i} \right] + \frac{1}{r_{12}} + BS_z, \quad (1)$$

where  $Z$  is the nuclear charge. The magnetic field is measured by the parameter  $\gamma = B/B_0$  with  $B_0 = 2.35 \times 10^5$  T. Here  $S_z = \sum_{i=1}^2 S_{z_i}$  is the  $z$  component of the total spin momentum, and serves as a good quantum number because the magnetic field is chosen to point in the  $z$  direction. In addition to  $S_z$ , the total spin angular momentum  $S$  and the  $Z$  parity  $\Pi_z = (-1)^{\sum_{i=1}^2 (l_i - m_i)}$  are also conserved quantities.

Upper bounds to energies of the atomic system in magnetic fields are calculated with the Rayleigh-Ritz variational method. In our calculations, the trial wave function is expanded in the form

$$\begin{aligned} \Psi(1,2) = & \sum_{ij} c_{ij} r_{12}^n [f_i(\rho_1, \varphi_1, z_1) g_j(\rho_2, \varphi_2, z_2) \\ & + f_j(\rho_2, \varphi_2, z_2) g_i(\rho_1, \varphi_1, z_1)] \frac{\alpha(1)\beta(2) - \alpha(2)\beta(1)}{\sqrt{2}}, \end{aligned} \quad (2)$$

where  $\alpha$  and  $\beta$  represent the spinor indices and  $c_{ij}$  is the expansion coefficient.  $f$  and  $g$  are the anisotropic Gaussian bases [22],

$$\phi_i(\rho, \varphi, z) = \rho^{n_{\rho i}} z^{n_{z i}} e^{-\alpha_i \rho^2 - \beta_i z^2} e^{im_i \varphi}, \quad i = 1, \dots, N, \quad (3)$$

where  $\alpha_i, \beta_i$  are positive nonlinear variational parameters and the exponents  $n_{\rho i}$  and  $n_{z i}$  obey the following restrictions:

TABLE I. Energies (in a.u.) for He of the  $1^10^+$  state obtained by the CI calculation with the use of different bases (G stands for the Gaussian basis and HG stands for the Hylleraas-Gaussian basis), and the contributions of every configuration in the absence of magnetic field ( $\Delta E$  stands for the contribution from every configuration, and  $E_T$  stands for the total energy using the configuration and all configurations listed before it).

Components	G		H-G		
	Number of terms	$\Delta E$	Number of terms	$\Delta E$	$E_T$
$0^+0^+$	794	-2.8912966537	738	-2.9217412111	-2.9010966802
$0^-0^-$	481	-0.0038479445	262	0.0064249943	-2.9021283939
$1^+-1^+$	481	-0.0077012456	262	0.0125466478	-2.9030684748
$1^-1^-$	436	-0.0002150292	172	-0.0002400294	-2.9032266534
$2^+-2^+$	436	-0.0002159723	172	-0.0003963290	-2.9033866318
$2^-2^-$	116	-0.0000209458	132	-0.0000350583	-2.9034312801
$3^+-3^+$	116	-0.0000204521	132	-0.0000319213	-2.9034729071
$3^-3^-$	100	-0.0000000013	100	-0.0000000008	-2.9034729078
$\gamma(L_z+2S_z)/2$		0.0000000000		0.0000000000	
Total	2960	-2.9033182444	1970	-2.9034729078	

$$n_{\rho i} = |m_i| + 2k_i, \quad k_i = 0, 1, 2, \dots$$

with  $m_i = \dots, -2, -1, 0, 1, 2, \dots$ ,

$$n_{z i} = \pi_{z i} + 2l_i, \quad l_i = 0, 1, 2, \dots \quad \text{with } \pi_{z i} = 0, 1. \quad (4)$$

The nonlinear variational parameters  $\alpha_i$  and  $\beta_i$  must be chosen carefully. In our work, a one-particle optimization procedure for H and He<sup>+</sup> is adopted to get two sets of  $\{\alpha_i^H, \beta_i^H\}$  and  $\{\alpha_j^{\text{He}}, \beta_j^{\text{He}}\}$ , and we also apply a direct two-particle optimization procedure to get another set of  $\{\alpha_i^{(1)}, \beta_i^{(1)}, \alpha_j^{(2)}, \beta_j^{(2)}\}$ . Both of the optimization procedures call a general downhill simplex subroutine, which is usually used in multidimension optimization.

The basis containing the  $r_{12}^n$  term and the Gaussian basis is called the Hylleraas-Gaussian basis. In this paper, only even powers of  $r_{12}$  are used in the trial wave function, so that the derivation of the matrix elements with the Gaussian basis (see the Appendixes in Refs. [22,23]) can be extended easily to the Hylleraas-Gaussian basis case after substituting  $r_{12}^n$  by a polynomial expansion of  $\rho$ ,  $z$ , and  $\varphi$ . We use the spectroscopic notation  $\nu^{2S+1}M^{I_z}$  to label the states of the helium atom in a magnetic field. In the notation,  $\nu$  stands for the degree of excitation, with respect to specified symmetry.

### III. RESULTS AND DISCUSSIONS

Table I shows the contributions of every configuration to the energy of the  $1^10^+$  state using the Hylleraas-Gaussian-type basis functions (HG in the table), and the corresponding contributions of every configuration using the Gaussian-type basis functions (G in the table) are also listed in the same table for comparison, both being in zero magnetic field. In our CI approach with the Gaussian basis, the ground-state energy is -2.903 318, which is worse than -2.903 351 in Ref. [22] because only 2960 terms are used. The ground-

state energy in our calculation with the Hylleraas-Gaussian-type basis is -2.903 473, about  $1.2 \times 10^{-4}$  below the relative data in Ref. [22]. It should be mentioned that, for the helium atom in zero magnetic field (a spherical symmetric case), one of the best nonrelativistic ground-state energies in theoretical calculations is -2.903 724 377 034 119 598 3 [27], and all the methods in cylindrical coordinates have an inherent limitation in attaining precision similar to that of the methods in spherical coordinates in the weak magnetic-field regime. All contributions in the calculation with the Gaussian basis are negative, but some of the contributions in the calculation with the Hylleraas-Gaussian basis are positive. The reason is that due to the introduction of  $r_{12}^n$ , the orthogonality between different configurations in the calculation with the Gaussian basis cannot be ensured in the calculation with the Hylleraas-Gaussian basis [for example, the  $(0^+, 0^+)$  configuration is not a ‘‘pure’’ configuration anymore, but a mixed one]. In the calculation with the Gaussian basis, the matrix element of the Zeeman term, as well as the total spin energy, is purely proportional to the corresponding overlap matrix element. Thus the Zeeman term and the total spin energy just give rise to a  $\gamma(L_z+2S_z)/2$  shift in the total energy. In the approach with the Hylleraas-Gaussian basis, there is a similar  $\gamma(L_z+2S_z)/2$  shift, which originates from a part of the Zeeman term [see Eq. (B5) in the Appendix] and the total spin energy.

For the  $\nu^10^+$  states, our strategy for choosing the combination of  $\alpha_i$ ,  $\beta_i$ , and  $r_{12}^n$  in each configuration can be demonstrated as  $\{\alpha_i^H, \beta_i^H, \alpha_j^{\text{He}}, \beta_j^{\text{He}}, r_{12}^0\}$ ,  $\{\alpha_i^{(1)}, \beta_i^{(1)}, \alpha_j^{(2)}, \beta_j^{(2)}, r_{12}^0\}$  and  $\{\alpha_i^{(1)}, \beta_i^{(1)}, \alpha_j^{(2)}, \beta_j^{(2)}, r_{12}^2\}$ , where the  $\{\alpha^{\text{H/He}}, \beta^{\text{H/He}}\}$  and  $\{\alpha_i^{(1)}, \beta_i^{(1)}, \alpha_j^{(2)}, \beta_j^{(2)}\}$  are nonlinear variational parameters obtained through the one- and two-particle optimization procedures, respectively. The direct two-particle optimization is a powerful step, and we can attain higher precision with relatively fewer terms. For the  $\nu^1(-1)^+$  and  $\nu^1(-2)^+$  states, the strategy for choosing  $\alpha_i$ ,  $\beta_i$ , and  $r_{12}^n$  is different, which can be

demonstrated as  $\{\alpha_i^H, \beta_i^H, \alpha_j^{\text{He}}, \beta_j^{\text{He}}, r_{12}^0\}$  and  $\{\alpha_i^H, \beta_i^H, \alpha_j^{\text{He}}, \beta_j^{\text{He}}, r_{12}^2\}$ . For the  $1^1 0^+$  state, the most contribution to the energy comes from the configurations with two antiparallel spin electrons in the same orbital, where the correlation between electrons is strong and the direct two-particle optimization procedure works with high efficiency. But for the  $\nu^1(-1)^+$  states, as well as the  $\nu^1(-2)^+$  states, the two-particle optimization procedure is not a necessary step anymore.

A detailed comparison between the numerical results for the energies of the  $\nu^1 0^+$ ,  $\nu^1(-1)^+$ , and  $\nu^1(-2)^+$  states, and the previously presented data for the energies is given in Table II. For the  $1^1 0^+$  state (our discussion is mainly about the state of  $\nu=1$ ), compared to the CI calculation with the Gaussian basis [22], our results are about  $1.0 \times 10^{-4}$  below in the weak magnetic-field regime, and about  $(3.0-5.0) \times 10^{-4}$  below in the intermediate and strong magnetic-field regime. For the  $1^1(-1)^+$  state, compared to the corresponding data in Ref. [23], our results are about  $(1.7-3.4) \times 10^{-5}$  below in the field regime of  $\gamma \leq 0.5$  a.u., and about  $(1.3-4.9) \times 10^{-4}$  below in the field regime of  $\gamma \geq 1.0$  a.u. For the  $1^1(-2)^+$  state, our results are very close to the relative data in Ref. [24] in the weak magnetic-field regime, and about  $(1.3-3.7) \times 10^{-4}$  below in the field regime of  $\gamma \geq 2.0$  a.u. Compared to the data using the Gaussian basis in cylindrical coordinates, our results are closer to the data obtained with the methods in other coordinate systems in Refs. [20,21]. It seems that the CI calculation with the Hylleraas-Gaussian basis is easier to yield high precision in strong magnetic fields.

As we know, the wave function of the helium atom goes to zero rapidly when the two electrons get close in space. The  $r_{12}^n$  term in the Hylleraas-Gaussian basis is a good consideration of the relative positions of electrons, which are not considered in the Gaussian basis. To fit the wave function, we need a large number of Gaussian basis functions in the trial wave function, but relatively fewer Hylleraas-Gaussian basis functions are needed due to the reason mentioned above. The total number of Hylleraas-Gaussian basis functions is not more than 2500 in the  $1^1 0^+$  case, while the typical number of Gaussian basis functions is 4378 in Ref. [22]. In the  $1^1(-1)^+$  and  $1^1(-2)^+$  cases, the total number of basis functions is about 3000–3500, which is similar to that of the basis functions used in Refs. [23,24] (about 3000–4000). For the  $1^1 0^+$  state, the Hylleraas-Gaussian basis is efficient (an increase of  $10^{-4}$  magnitude in precision compared to the corresponding results of the CI calculation with the Gaussian basis) through the whole region of  $\gamma=0-100$  a.u. For other states in our calculation, the Hylleraas-Gaussian basis is highly efficient when the magnetic-field strength is not too weak [ $\gamma \geq 1.0$  a.u. for the  $1^1(-1)^+$  state and  $\gamma \geq 2.0$  a.u. for the  $1^1(-2)^+$  state]. Figure 1 shows the variation of the average value of  $r_{12}$  as a function of the magnetic-field strength. While the magnetic-field strength increases, the average value of  $r_{12}$  decreases monotonically. At the points of  $\gamma = 1.0$  a.u. in the curve of  $1^1(-1)^+$  and  $\gamma = 2.0$  a.u. in the curve of  $1^1(-2)^+$ , the average values of  $r_{12}$  are 4.4835 and 4.3833 a.u., respectively. We can draw an initial conclusion that the Hylleraas-Gaussian basis is more efficient when the average value of  $r_{12}$  is less than about 4.5 a.u., and better results can be attained in the strong magnetic-field regime.

#### IV. CONCLUSION

In the present work, we apply a CI method based on the Hylleraas-Gaussian basis functions to the computation of the helium atom in strong magnetic fields. Compared to the CI method with the Gaussian basis [22–24], our method is more efficient with the average value of  $r_{12}$  less than 4.5 a.u., and it is satisfied for all states we discussed in the strong magnetic-field regime. The reason for the improvement in precision is that the Hylleraas-Gaussian basis functions take into consideration the relative positions of electrons, with which the trial wave function goes to zero rapidly when the electrons get close in space, and thus we can fit the real wave function better. In the case of  $r_{12} \gg 4.5$  a.u., it maybe helpful to add another  $e^{-\pi r_{12}^2}$  term to the trial wave function in Eq. (2), which makes the trial wave function go to zero rapidly while  $r_{12}$  increases. As the dimension of the general eigenvalue problem is not more than 4000, all our calculations have been carried out on a personal computer (2.53 GHz  $\times$  2 CPU and 2 GB RAM).

#### APPENDIX A: THE OVERLAP MATRIX ELEMENTS

As discussed above, our work is a simple but effective extension of the computational approach of Becken and Schmelcher (see Refs. [22,23], and the appendixes therein). The trial wave function in Eq. (2) can be expressed as

$$\Psi(1,2) = \sum_{ij} c_{ij} \Psi_{ij}. \quad (\text{A1})$$

For the overlap matrix elements, a straightforward calculation leads to

$$\langle \Psi_{ij} | \Psi_{kl} \rangle = \langle \phi_{ij} | \phi_{kl} \rangle + \langle \phi_{ij} | \phi_{lk} \rangle, \quad (\text{A2})$$

where  $\langle \phi_{ij} | \phi_{kl} \rangle$  ( $\langle \phi_{ij} | \phi_{lk} \rangle$  has a similar equation) is an integration over the whole space and leads to the following after a few steps of algebra:

$$\begin{aligned} \langle \phi_{ij} | \phi_{kl} \rangle &= \int d\vec{r}_1 d\vec{r}_2 r_{12}^{2n} \rho_1^{n_{\rho_{ik}}} z_1^{n_{z_{ik}}} e^{-\alpha_{ik} \rho_1^2 - \beta_{ik} z_1^2} e^{-i(m_i - m_k) \varphi_1} \\ &\quad \times \rho_2^{n_{\rho_{jl}}} z_2^{n_{z_{jl}}} e^{-\alpha_{jl} \rho_2^2 - \beta_{jl} z_2^2} e^{-i(m_j - m_l) \varphi_2} \\ &= \pi^2 \delta_{m_{ij}, m_{kl}} \sum_{\substack{s_1 + s_2 + \dots + s_6 = n \\ k_0 + k_1 = s_3}} \binom{n}{s_1 s_2 \dots s_6} \binom{s_3}{k_0 k_1} \\ &\quad \times \delta_{m_{i+k_0}, m_{j+k_1}} g_{n_{z_{ik}} + 2s_4 + s_6 + 1} g_{n_{z_{jl}} + 2s_5 + s_6 + 1} (-1)^{s_3} (-2)^{s_6} \\ &\quad \times \alpha_{ik}^{-n_{\rho_{ik}} + 2s_1 + s_3 + 2/2} \alpha_{jl}^{-n_{\rho_{jl}} + 2s_2 + s_3 + 2/2} \beta_{ik}^{-n_{z_{ik}} + 2s_4 + s_6 + 1/2} \\ &\quad \times \beta_{jl}^{-n_{z_{jl}} + 2s_5 + s_6 + 1/2} \Gamma\left(\frac{n_{\rho_{ik}} + 2s_1 + s_3 + 2}{2}\right) \\ &\quad \times \Gamma\left(\frac{n_{\rho_{jl}} + 2s_2 + s_3 + 2}{2}\right) \Gamma\left(\frac{n_{z_{ik}} + 2s_4 + s_6 + 1}{2}\right) \\ &\quad \times \Gamma\left(\frac{n_{z_{jl}} + 2s_5 + s_6 + 1}{2}\right), \end{aligned} \quad (\text{A3})$$

TABLE II. Energies (in a.u.)  $E$  and previously presented results for the total energies ( $E_{\text{lit}}^{a,b,c}$  are the results in cylindrical coordinates and  $E_{\text{lit}}^{d,e}$  are the results in other coordinate systems) at different field strengths for the states of  $\nu^1 0^+$ ,  $\nu^1(-1)^+$ , and  $\nu^1(-2)^+$  ( $\nu=1, 2$ ).

$\gamma$	$1^1 0^+$			$2^1 0^+$			$1^1(-1)^+$			$2^1(-1)^+$			$1^1(-2)^+$		
	$E$	$E_{\text{lit}}^a$	$E_{\text{lit}}$	$E$	$E_{\text{lit}}^a$	$E_{\text{lit}}$	$E$	$E_{\text{lit}}^b$	$E_{\text{lit}}$	$E$	$E_{\text{lit}}^b$	$E_{\text{lit}}^d$	$E$	$E_{\text{lit}}^c$	$E_{\text{lit}}^d$
0	-2.903473	-2.903351	-2.90372 <sup>d</sup>	-2.145951	-2.145912	-2.14597 <sup>d</sup>	-2.123801	-2.123774	-2.12384 <sup>d</sup>	-2.055131	-2.055124	-2.05514	-2.055619		-2.05562
			-2.903724 <sup>e</sup>			-2.145974 <sup>e</sup>			-2.12379 <sup>e</sup>				-2.055619		
0.01	-2.903451		-2.903704 <sup>e</sup>	-2.145683		-2.145706 <sup>e</sup>	-2.128490		-2.12848 <sup>e</sup>	-2.058360			-2.064304		
0.02	-2.903386	-2.903270	-2.903645 <sup>e</sup>	-2.144883	-2.144852	-2.144913 <sup>e</sup>	-2.132561	-2.132539	-2.13254e	-2.058629	-2.058622		-2.070727	-2.070739	
0.05	-2.902966			-2.139616			-2.141515			-2.050363			-2.081843		
0.1	-2.901479		-2.901740 <sup>e</sup>	-2.123512		2.123553 <sup>e</sup>	-2.148464		-2.14846 <sup>e</sup>	-2.029861			-2.087439		
0.2	-2.895499		-2.89583 <sup>d</sup>	-2.076450		-2.07650 <sup>d</sup>	-2.145196		-2.14527 <sup>d</sup>	-1.987779		-1.98828	-2.079374		-2.07949
0.5	-2.855906	-2.855859		-1.908712	-1.908671		-2.077346	-2.077302		-1.843347	-1.843343		-2.000892	-2.000873	
1	-2.730015	-2.729508	-2.73038 <sup>d</sup>	-1.617892	-1.617870	-1.61787 <sup>e</sup>	-1.885011	-1.884875		-1.565704	-1.565692		-1.798998	-1.798963	
			-2.730373 <sup>e</sup>												
2	-2.330270	-2.329780	-2.33065 <sup>e</sup>	-0.975874	-0.975861		-1.369122	-1.368986		-0.930512	-0.930508		-1.272606	-1.272473	
5	-0.575411	-0.574877	-0.5755 <sup>e</sup>	1.252364	1.252363		0.619038	0.619265		1.291508	1.291512		0.734027	0.734276	
10	3.064202	3.064582		5.393203	5.3932		4.500762	4.500982		5.428068	5.428064		4.636247	4.636327	
20	11.266617	11.267051		14.249009	14.248991		13.010161	13.010551		14.27984	14.279839		13.174041	13.174417	
50	38.07607	38.07632		42.207553	42.20751		40.339265	40.339488		42.233622	42.233602		40.558421	40.558628	
100	84.918049	84.918313		90.180739	90.18069		87.670794	87.671288		90.203624	90.203618		87.949409	87.949762	

<sup>a</sup>Reference [22].

<sup>b</sup>Reference [23].

<sup>c</sup>Reference [24].

<sup>d</sup>Reference [20].

<sup>e</sup>Reference [21].

where  $(\begin{smallmatrix} n \\ s_1 s_2 \dots s_6 \end{smallmatrix})$  and  $(\begin{smallmatrix} s_3 \\ k_0 k_1 \end{smallmatrix})$  are the polynomial coefficients, and  $g_l = \text{mod}(l, 2)$ .

There are two key steps in this derivation, the first being the following substitution [23]:

$$\varphi = \varphi_1 - \varphi_2, \quad \bar{\varphi} = \frac{1}{2}(\varphi_1 + \varphi_2). \quad (\text{A4})$$

The integrations about  $\varphi_1$  and  $\varphi_2$  are converted to the integrations about  $\varphi$  and  $\bar{\varphi}$ , which eventually lead to the product of two Kronecker delta functions. The next step is to expand  $r_{12}^{2n}$  as

$$r_{12}^{2n} = [\rho_1^2 + \rho_2^2 - 2\rho_1\rho_2 \cos \varphi + z_1^2 + z_2^2 - 2z_1z_2]^n, \quad (\text{A5})$$

and the corresponding expansion coefficients are  $s_1, s_2, \dots, s_6$ . The integrations about  $\rho$  and  $z$  have a Gaussian-type form ( $\int x^n e^{-bx^2} dx$ ), and can be calculated explicitly.

## APPENDIX B: THE HAMILTONIAN MATRIX ELEMENTS

The matrix elements of the operator  $\frac{1}{2}(p + \frac{1}{2}\mathbf{B} \times \mathbf{r})^2$  can be expressed in cylindrical coordinates as

$$\begin{aligned} \frac{1}{2}\left(p + \frac{1}{2}\mathbf{B} \times \mathbf{r}\right)^2 &= -\frac{1}{2}\left[\left(\frac{\partial^2}{\partial \rho^2} + \frac{1}{\rho}\frac{\partial}{\partial \rho}\right) + \frac{1}{\rho^2}\frac{\partial^2}{\partial \varphi^2} + \frac{\partial^2}{\partial z^2}\right. \\ &\quad \left.+ iB\frac{\partial}{\partial \varphi} - \frac{1}{4}B^2\rho^2\right] \\ &= T_\rho + T_\varphi + T_z + T_{\text{Zeeman}} + T_{\text{dia}}, \end{aligned} \quad (\text{B1})$$

where  $T_\rho$ ,  $T_\varphi$ , and  $T_z$  represent the Laplacian, and  $T_{\text{Zeeman}}$  and  $T_{\text{dia}}$  are the Zeeman term and the diamagnetic term, respectively.

After a few steps of partial integration,  $\langle \phi_{ij} | T_\rho | \phi_{kl} \rangle$  changes to a symmetric form as below (the integrations about other variables are the same as the derivation in Appendix A and are omitted here).

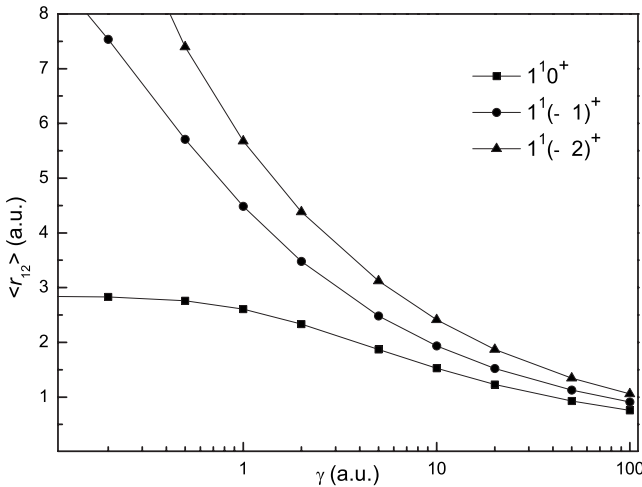


FIG. 1. Average value of  $r_{12}$  for the  $1^1 0^+$ ,  $1^1(-1)^+$ , and  $1^1(-2)^+$  states as a function of the magnetic-field strength.

$$\begin{aligned} \langle \phi_{ij} | T_{\rho_1} | \phi_{kl} \rangle &= \frac{1}{2} \int_0^\infty \rho_1 \phi'_{ij} \phi'_{kl} d\rho_1 \\ &= \frac{1}{2} \int_0^\infty \rho_1^{n_{\rho_{ik}}} r_{12}^{2n} e^{-\alpha_{ik} \rho_1^2} \left\{ -2n_{\rho_k} \alpha_i - 2n_{\rho_i} \alpha_k \right. \\ &\quad \left. + \frac{n_{\rho_i} n_{\rho_k}}{\rho_1^2} + 4\alpha_i \alpha_k \rho_1^2 \right. \\ &\quad \left. + \frac{1}{r_{12}^2} \left[ 2(n_{kl} n_{\rho_i} + n_{ij} n_{\rho_k}) \left( 1 - \frac{\cos \varphi \rho_2}{\rho_1} \right) \right. \right. \\ &\quad \left. \left. - 4(n_{kl} \alpha_i + n_{ij} \alpha_k) (\rho_1^2 - \cos \varphi \rho_1 \rho_2) \right] \right. \\ &\quad \left. + \frac{1}{r_{12}^4} 4n_{ij} n_{kl} (\rho_1^2 - 2 \cos \varphi \rho_1 \rho_2 \right. \\ &\quad \left. + \rho_2^2 \cos^2 \varphi) \right\} \rho_1 d\rho_1. \end{aligned} \quad (\text{B2})$$

Similar to Eq. (A3), every term in  $\langle \phi_{ij} | T_\rho | \phi_{kl} \rangle$  can be evaluated separately. The expressions of the matrix elements of  $T_\varphi$ ,  $T_z$ ,  $T_{\text{Zeeman}}$ , and  $T_{\text{dia}}$  are listed in Eqs. (B3)–(B6).

$$\begin{aligned} \langle \phi_{ij} | T_{\varphi_1} | \phi_{kl} \rangle &= \frac{1}{2} \int_0^{2\pi} \frac{\phi_{ij}^* \phi_{kl}'}{\rho_1^2} d\varphi_1 \\ &= \frac{1}{2} \int_0^{2\pi} r_{12}^{2n} e^{i(m_k - m_i) \varphi_1} \left[ \frac{m_i m_k}{\rho_1^2} + \frac{1}{r_{12}^2} 2(m_k n_{ij} \right. \\ &\quad \left. - m_i n_{kl}) \frac{i \rho_2 \sin \varphi}{\rho_1} \right. \\ &\quad \left. + \frac{1}{r_{12}^4} 4n_{ij} n_{kl} \rho_2^2 \sin^2 \varphi \right] d\varphi_1, \end{aligned} \quad (\text{B3})$$

$$\begin{aligned} \langle \phi_{ij} | T_{z_1} | \phi_{kl} \rangle &= \frac{1}{2} \int_{-\infty}^{+\infty} \phi_{ij}' \phi_{kl}' dz_1 \\ &= \frac{1}{2} \int_{-\infty}^{+\infty} z_1^{n_{z_{ik}}} r_{12}^{2n} e^{-\beta_{ik} z_1^2} \left\{ -2n_{z_k} \beta_i - 2n_{z_i} \beta_k \right. \\ &\quad \left. + \frac{n_{z_i} n_{z_k}}{z_1^2} + 4\beta_i \beta_k z_1^2 + \frac{1}{r_{12}^2} \left[ 2(n_{kl} n_{z_i} + n_{ij} n_{z_k}) \right. \right. \\ &\quad \left. \left. \times \left( 1 - \frac{z_2}{z_1} \right) - 4(n_{kl} \beta_i + n_{ij} \beta_k) (z_1^2 - z_1 z_2) \right] \right. \\ &\quad \left. + \frac{1}{r_{12}^4} 4n_{ij} n_{kl} (z_1^2 - 2z_1 z_2 + z_2^2) \right\} dz_1, \end{aligned} \quad (\text{B4})$$



$$\begin{aligned}
\langle \phi_{ij} | T_{\text{Zeeman}} | \phi_{kl} \rangle &= -\frac{1}{2} \int_0^{2\pi} iB \phi_{ij}^* \phi'_{kl} d\varphi_1 \\
&= \frac{1}{2} \int_0^{2\pi} r_{12}^{2n} e^{i(m_k - m_i)\varphi_1} \\
&\quad \times B \left[ -\frac{\rho_1 \rho_2 (i \sin \varphi) 2n_{kl}}{r_{12}^2} + m_k \right] d\varphi_1 \\
&= -\frac{B}{2} \int_0^{2\pi} r_{12}^{2n} e^{i(m_k - m_i)\varphi_1} \\
&\quad \times \frac{2n_{kl} \rho_1 \rho_2 (i \sin \varphi)}{r_{12}^2} d\varphi_1 + \frac{m_k B}{2} \langle \phi_{ij} | \phi_{kl} \rangle, \tag{B5}
\end{aligned}$$

$$\langle \phi_{ij} | T_{\text{dia1}} | \phi_{kl} \rangle = \frac{1}{2} \int_0^\infty \frac{1}{4} B^2 \rho_1^2 d\rho_1. \tag{B6}$$

The second part on the right side of Eq. (B5) is proportional to the corresponding overlap matrix element. Thus this part in the Zeeman term and the total spin energy just give rise to a  $\gamma(L_z + 2S_z)/2$  shift in the total energy.

The evaluation of the matrix elements of the electronic Coulomb interaction with the nucleus is a little complicated. First, we apply a Singer transformation [28]

$$\frac{1}{r_1} = \frac{2}{\sqrt{\pi}} \int_0^\infty e^{-u^2 r_1^2} du. \tag{B7}$$

After a few steps of algebra, we obtain

$$\begin{aligned}
\left\langle \phi_{ij} \left| \frac{1}{r_1} \right| \phi_{kl} \right\rangle &= \cdots \int_0^\infty \frac{2}{\sqrt{\pi}} \left( 1 + \frac{1}{\alpha_{ik}} u^2 \right)^{-(n_{\rho_{ik}} + 2s_1 + s_3 + 2)/2} \\
&\quad \times \left( 1 + \frac{1}{\beta_{ik}} u^2 \right)^{-n_{z_{ik}} + 2s_4 + s_6 + 1/2} du \dots, \tag{B8}
\end{aligned}$$

where the ellipsis stands for the same terms as the overlap matrix elements in Eq. (A3), and we only need to add this integration (which can be calculated explicitly by using the hypergeometric functions) to the inner integration (or inner loop) in Eq. (A3).

The evaluation of the matrix elements of the interaction between electrons is much more complicated, and we only give the final expression here:

$$\begin{aligned}
\left\langle \phi_{ij} \left| \frac{1}{r_{12}} \right| \phi_{kl} \right\rangle &= 2\pi \sqrt{\pi} \delta_{m_{ij}, m_{kl}} \sum \binom{n}{s_1 \cdots s_6} \binom{|m_j|}{k_0 \ k_1} \binom{|m_l|}{k_2 \ k_3} \binom{s_2 + k_{jl}}{k_4 \ k_5 \ k_6} \binom{s_3}{k_7 \ k_8} \binom{n_{z_{ij}} + 2s_5 + s_6}{t_1 \ t_2} \binom{k_6 + k_7}{t_3 \ t_4} \\
&\quad \times \delta[k_0 \operatorname{sgn}(m_j) + t_3, k_2 \operatorname{sgn}(m_l) + t_4] g(n_{z_{ik}} + 2s_4 + s_6 + t_2 + 1) g(t_1 + 1) (-1)^{s_3} (-2)^{s_6} 2^{k_8} \\
&\quad \times \Gamma(\text{ex1}) \Gamma(\text{ex2}) \Gamma(\text{ex3}) \Gamma(\text{ex4}) (\alpha_{ik} \alpha_{jl})^{-\text{ex1}} (\beta_{ik} \beta_{jl})^{-\text{ex3}} \\
&\quad \times \sum \binom{n_{\rho_{ik}} + 2s_1 - n_{\rho_{jl}} - 2s_2}{n_1 n_2} \binom{n_{z_{ik}} + 2s_4 - n_{z_{jl}} - 2s_5}{n_3 n_4} \\
&\quad \times \int_0^\infty (u^2)^{k_1 + k_3 + 2k_5 + k_8 + t_2 + n_4} \left( 1 + \frac{\alpha_{ijkl}}{\alpha_{ik} \alpha_{jl}} u^2 \right)^{-\text{ex1}} \left( 1 + \frac{\beta_{ijkl}}{\beta_{ik} \beta_{jl}} u^2 \right)^{-\text{ex3}} du, \tag{B9}
\end{aligned}$$

where

$$\begin{aligned}
\text{ex1} &= \frac{n_{\rho_{ik}} + 2s_1 + s_3 + k_1 + k_3 + 2k_5 + k_6 + k_8 + 2}{2}, \\
\text{ex2} &= \frac{k_0 + k_2 + 2k_4 + k_6 + k_7 + 2}{2}, \\
\text{ex3} &= \frac{n_{z_{ik}} + 2s_4 + s_6 + t_2 + 1}{2}, \quad \text{ex4} = \frac{t_1 + 1}{2}. \tag{B10}
\end{aligned}$$

The integration about variable  $u$  in Eq. (B9) can also be evaluated by using the hypergeometric functions. Equation (B9) is adopted for the case of  $n_{\rho_{ik}} + 2s_1 \geq n_{\rho_{jl}} + 2s_2$  and  $n_{z_{ik}}$

$+ 2s_4 \geq n_{z_{jl}} + 2s_5$ . For the other case, exchanges of parameters as follows should be made:

$$\begin{aligned}
\text{for } n_{\rho_{jl}} + 2s_2 > n_{\rho_{ik}} + 2s_1, \quad n_{\rho_{jl}} \leftrightarrow n_{\rho_{ik}} \quad s_2 \leftrightarrow s_1 \quad \alpha_{jl} \leftrightarrow \alpha_{ik}, \\
\text{for } n_{z_{jl}} + 2s_5 > n_{z_{ik}} + 2s_4, \quad n_{z_{jl}} \leftrightarrow n_{z_{ik}} \quad s_5 \leftrightarrow s_4 \quad \beta_{jl} \leftrightarrow \beta_{ik}. \tag{B11}
\end{aligned}$$

The key steps are the Singer transformation [28] of  $1/r_{12} = 2/\sqrt{\pi} \int_0^\infty e^{-u^2 r_{12}^2} du$  and a series of variable substitutions (similar to the Appendix in Ref. [23]).

### APPENDIX C: THE HYPERGEOMETRIC FUNCTIONS

The integrations about  $u$  in Eqs. (B8) and (B9) can be evaluated explicitly by using the hypergeometric functions.

After a transformation from  $u$  to  $x$  ( $u^2=x/[a_1(1-x)]$ ), the upper limit of integral changes from infinity to 1,

$$\begin{aligned} & \int_0^\infty (u^2)^{b_1}(1+a_1u^2)^{-b_2}(1+a_2u^2)^{-b_3}du \\ &= \frac{1}{2}a_1^{-b_1-(1/2)} \int_0^1 x^{b_1-(1/2)}(1-x)^{b_2+b_3-b_1-(3/2)} \\ & \quad \times \left(1 - \frac{a_1-a_2}{a_1}x\right)^{-b_3} dx. \end{aligned} \quad (\text{C1})$$

The right side of Eq. (C1) can be calculated with a hypergeometric function and gamma functions

$$\begin{aligned} F(\alpha, \beta, \gamma, z) &= \frac{\Gamma(\gamma)}{\Gamma(\beta)\Gamma(\gamma-\beta)} \int_0^1 t^{\beta-1}(1-t)^{\gamma-\beta-1}(1-zt)^{-\alpha} \\ & \quad \times dt (\gamma > \beta > 0). \end{aligned} \quad (\text{C2})$$

It is easy to testify that the condition of  $\gamma > \beta > 0$  is ensured in Eqs. (B8) and (B9). We use a HYGFX subroutine in the general special-function package to evaluate the hypergeometric functions quickly and explicitly.

- 
- [1] J. Truemper, W. Pietsch, C. Reppin, W. Voges, R. Staubert, and E. Kendziorra, *Astron. J.* **219**, L105 (1978).  
 [2] R. J. Elliott and R. Loudon, *J. Phys. Chem. Solids* **15**, 196 (1960).  
 [3] Y. Wan, G. Ortiz, and P. Phillips, *Phys. Rev. Lett.* **75**, 2879 (1995).  
 [4] W. Rösner, G. Wunner, H. Herold, and H. Ruder, *J. Phys. B* **17**, 29 (1984).  
 [5] H. Ruder, G. Wunner, H. Herold, and F. Geyer, *Atoms in Strong Magnetic Fields* (Springer, Berlin, 1994).  
 [6] H. Friedrich, *Phys. Rev. A* **26**, 1827 (1982).  
 [7] D. Wintgen and H. Friedrich, *J. Phys. B* **19**, 991 (1986).  
 [8] M. V. Ivanov, *J. Phys. B* **21**, 447 (1988).  
 [9] J. Shertzer, *Phys. Rev. A* **39**, 3833 (1989).  
 [10] J. Xi, L. Wu, X. He, and B. Li, *Phys. Rev. A* **46**, 5806 (1992).  
 [11] D. S. Chuu and Y. K. Lee, *Phys. Rev. A* **48**, 4175 (1993).  
 [12] J. X. Zang and M. L. Rustgi, *Phys. Rev. A* **50**, 861 (1994).  
 [13] J. H. Wang and C. S. Hsue, *Phys. Rev. A* **52**, 4508 (1995).  
 [14] Y. P. Kravchenko, M. A. Liberman, and B. Johansson, *Phys. Rev. A* **54**, 287 (1996).  
 [15] P. Schmelcher and W. Schweizer, *Atoms and Molecules in Strong External Fields* (Springer, Berlin, 1998).  
 [16] A. Rutkowski and A. Poszwa, *Phys. Rev. A* **67**, 013412 (2003).  
 [17] R. F. Green and J. Liebert, *Publ. Astron. Soc. Pac.* **93**, 105 (1981).  
 [18] G. D. Schmidt, W. B. Latter, and C. B. Foltz, *Astrophys. J.* **350**, 758 (1990).  
 [19] M. V. Ivanov, *J. Phys. B* **27**, 4513 (1994).  
 [20] A. Scrinzi, *Phys. Rev. A* **58**, 3879 (1998).  
 [21] M. Hesse and D. Baye, *J. Phys. B* **32**, 5605 (1999).  
 [22] W. Becken, P. Schmelcher, and F. K. Diakonou, *J. Phys. B* **32**, 1557 (1999).  
 [23] W. Becken and P. Schmelcher, *J. Phys. B* **33**, 545 (2000).  
 [24] W. Becken and P. Schmelcher, *Phys. Rev. A* **63**, 053412 (2001).  
 [25] S. Jordan, P. Schmelcher, W. Becken, and W. Schweizer, *Astron. Astrophys.* **336**, L33 (1998).  
 [26] S. Jordan, P. Schmelcher, and W. Becken, *Astron. Astrophys.* **376**, 614 (2001).  
 [27] G. W. F. Drake, M. M. Cassar, and R. A. Nistor, *Phys. Rev. A* **65**, 054501 (2002).  
 [28] K. Singer, *Proc. R. Soc. London, Ser. A* **402**, 412 (1960).